Estimation of the Surface Velocity Field of Temperate Glaciers Using Airborne SAR Interferometry.

Pau Prats, Christian Andres, Rolf Scheiber, Andreas Reigber and Ralf Horn
German Aerospace Center (DLR), Germany

Abstract

This paper presents a methodology to process airborne interferometric SAR data to measure surface velocity fields of temperate glaciers. First, a solution based on multi-squint is proposed to estimate residual motion errors (inaccuracies of the navigation system on the order of a few centimeters) in the case of non-stationary scenes. Afterwards, an efficient methodology to derive surface velocity fields with airborne systems is expounded, where the line-of-sight displacement is estimated using differential interferometry, and the along-track component by estimating the azimuth coregistration offsets. The necessary steps to finally obtain the 3D surface velocity field are also presented, as well as the possibility to combine different acquisition geometries. Airborne interferometric SAR data acquired by the Experimental SAR system of DLR over the Aletsch glacier, located in the Swiss Alps, are used to evaluate the performance of the proposed approach.

1 Introduction

The monitoring of alpine glaciers is essential to predict their evolution under the threat of global warming. However, the data is often scarce covering a few glaciers, given the difficulties to make field measurements in such high altitude and remote scenarios. A solution is provided by remotely sensed SAR data, which offers the possibility to obtain surface velocity fields (SVF) of glaciers within wide areas and with high accuracy. This information can be used within ice flow models to derive the ice thickness of the glacier [1]. In particular, differential SAR interferometry (DInSAR) is a well-known technique to measure surface subsidence/motion for a wide range of applications: modeling surface deformation, landslides, soil compaction rate, atmosphere estimation and glacier monitoring, among others. Spaceborne SAR systems have already proven the possibility to measure SVF [2, 3], but the lack of flexibility in the acquisition configuration as well as the fixed, and usually too large, re-visit time, can become a limitation in many cases. Airborne SAR systems offer an excellent opportunity to overcome the limitations of spaceborne sensors given their inherent flexibility in the sense of data acquisition geometry and used wavelength, not to mention their higher spatial resolution. However, the processing of airborne data is not as straightforward as in the spaceborne case. The fact that the platform does not follow an ideal linear trajectory does not turn out to be a problem itself, since efficient motion compensation (MoCo) is possible [6, 7]. However, the main drawback is the existence of the so-called *residual motion errors* (RME): inaccuracies in the navigation data in the order of a few centimeters. Such azimuth varying errors can strongly limit the accuracy of the obtained interferograms, masking completely the motion to be measured.

This paper presents SVF derived from airborne SAR interferometry. Section 2 revisits the extended multi-squint (EMS) approach presented in [8] to estimate RME in non-stationary scenes. Section 3 focuses on the estimation of SVF of temperate glaciers using multi-baseline airborne SAR interferometry. All the necessary processing steps are discussed, including also the retrieval of the 3D SVF and the combination of different configurations. Finally, Section 4 evaluates the performance of the proposed approach using airborne data acquired by the Experimental SAR (E-SAR) system of DLR in the frame of the SWISAR campaign. The data were acquired at X-, C-, L- and P-band over the Aletsch glacier of the Swiss Alps in the years 2003 and 2006.

2 Extended Multi-Squint

This section describes the retrieval of relative residual motion errors, i.e. baseline errors, in the presence of a non-stationary scene. The effects of RME and a real azimuth displacement of the scene between the acquisitions, from now on called a *true coregistration error* (TCE), are similar, resulting in azimuth coregistration offsets. Therefore, the separation of these two effects can become problematic. In [8] it was shown that it is possible to decouple both contributions on a pixel-by-pixel basis with the EMS approach, whose block diagram is shown in **Figure 1**. From the N looks, $N-1$ spectral diversity (SD) phases can be generated. The proposed solution in order to separate the derivative of the baseline error from the TCE is to take the difference between two adjacent SD phases. Doing so, the TCE will be completely removed. The retrieved $N-2$ differential SD phases are related to the second derivative of the baseline error, so that after aligning and adding them in the complex domain a model-based inversion based on a LS solution as presented in [4] is carried out to retrieve the second derivative of the horizontal $\ddot{\epsilon}_{\mathrm{y}}(x)$ and vertical $\ddot{\epsilon}_{\mathrm{z}}(x)$ baseline error. Finally, a two step integration yields the desired solution.

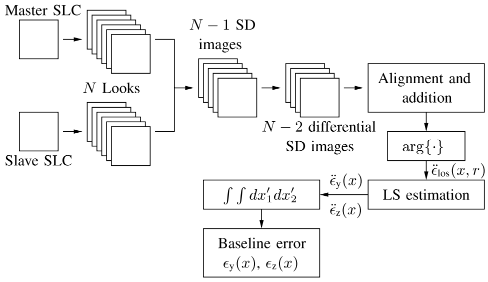

Figure 1: Block diagram of the EMS approach

Once the baseline error is estimated, the track of the slave image can be updated with ϵ_{y} and ϵ_{z}, so that both images will have the same RME after re-processing, hence canceling out after interferogram generation. Finally, any azimuth coregistration error in the scene will correspond to a TCE, which can be efficiently estimated using SD [5].

3 Methodology to Retrieve SVF with Airborne Interferometric SAR

The previous section dealt with the particularities of airborne systems in repeat-pass scenarios, where RME must be compensated. This section presents the methodology to retrieve the 3D SVF using multi-baseline airborne SAR interferometry, as several steps must be carried out in order to retrieve reliable displacement information in the airborne case. In particular, the classical three image DInSAR approach is used to retrieve the LOS displacement, where two images are acquired the same day and a third one (the long-term slave) is acquired after the event. In addition, the along-track displacement is retrieved by estimating the azimuth offsets between the master image and the long-term slave using the spectral diversity (SD) technique. The different steps to retrieve the 3D SVF are commented next:

Pre-processing: In order to ease the forthcoming interferometric processing several issues should be considered. On the one hand, the reference tracks should be parallel and with the same azimuth sampling for the three acquisitions. Doing so, the images will be automatically aligned along the azimuthal dimension, but for the existence of RME and TCE. On the other hand, the strong topography present in the scene must be considered during motion compensation (MoCo). The assumption of a constant reference height, which is the standard approach when focusing SAR data using Fourier-based processing algorithms [6], can introduce severe phase and azimuth coregistration errors in repeat-pass scenarios. Therefore, an external DEM is mandatory, taking into account that its accuracy and resolution will have a direct impact on the accuracy of the retrieved SVF. There are several possibilities in order to take into account the topography, from time-domain approaches until topography- and aperture-dependent (TAD) MoCo algorithms [7]. With the use of the reference tracks the external DEM is back-geocoded to the azimuth/slant-range plane.

SAR Processing: The raw data are focused using the Extended Chirp Scaling (ECS) algorithm with the integrated two-step motion compensation [6], while the sub-aperture topography- and aperture-dependent (SATA) algorithm and the precise topography- and aperture-dependent (PTA) algorithm have been selected as TAD algorithms to accommodate the strong topography of the scene [7].

Estimation of the Baseline Error: The conventional MS approach is used with the short-term interferogram, while the EMS algorithm is used with the long-term one. Afterwards, the slave tracks are updated with their corresponding baseline errors and re-processed.

Interferometric Processing: A conventional interferometric processing is carried out. First, the range coregistration offsets computed from the external DEM are used to carry out the range interpolation for both slaves. The interferogram can now be generated for the short-term pair, as no TCE is present. However, SD is applied in both dimensions to estimate the TCE in the long-term interferogram. The retrieved offsets are used to further correct the coregistration values of the long-term slave. Finally, the long-term interferogram is generated, and a classical three image DInSAR approach is performed in order to estimate the LOS displacement. Together with the along-track displacement estimated before with SD, the 2D SVF of the glacier in the azimuth/slant-range plane is retrieved. It should be stressed that due to the azimuth-varying baseline of airborne systems, the real track deviations should be used to compute the height sensitivity, which is used to scale the residual interferometric phases during the DInSAR processing [9].

Retrieval of the 3D SVF: Once the 2D SVF has been estimated, it is then possible to retrieve the 3D one after making some assumptions, since for every pixel only two measurements are available, but there are three unknowns for the displacement. This can be solved by assuming that the glacier flows in the direction of the maximum slope, and that there is no emergence/submergence subsidence (surface parallel flow assumption) [2]. With the external DEM it is possible to estimate the depression angle and orientation of the slope, yielding the direction of the movement, so that only the magnitude of the displacement M is unknown. The solution can be retrieved via weighted least-squares (WLS) estimation.

A last step involves converting the retrieved 3D SVF, which is in the azimuth/slant-range plane, to a global reference system, e.g. WGS-84 or Universal Transverse Mercator (UTM). It is worth commenting that the intrinsic flexibility of an airborne platform allows acquiring multiple acquisitions in a short time frame. Therefore, several tracks can be flown in order to retrieve different projections of the displacement, and consequently obtain a better estimation of the SVF. In fact, with one more pair of measurements, e.g. acquired in a track perpendicular to the previous one, it is possible to avoid any assumption concerning the direction of the glacier motion, hence estimating directly the three components of the displacement vector using also a WLS estimation.

4 Experimental Results

Data acquired by the Experimental SAR (E-SAR) system of the German Aerospace Center (DLR) are used to validate the proposed approach. The data were acquired over the Aletsch glacier, located in the Swiss Alps, in the frame of the SWISAR campaign, in the years 2003 and 2006. Several data takes were performed in P-, C-, L-, and X-band, but only P- and L-band were acquired on two consecutive days in order to perform differential interferometry. The configuration acronyms stand for *Fieschersattel* (FISA) and *Jungfraujoch* (JUJO).

After applying the processing chain expounded in Section 3 to each group of images, several SVF were retrieved. **Figure 2** shows the estimated along-track and LOS displacements with the corresponding 2D SVF for the 2003 campaign in the FISA configuration, while **Figure 3** shows the result for 2006. From the 2D SVF it is clear that the along-track information is very valuable, since in some areas the DInSAR measurement cannot yield any estimation due to the lack of movement in LOS.

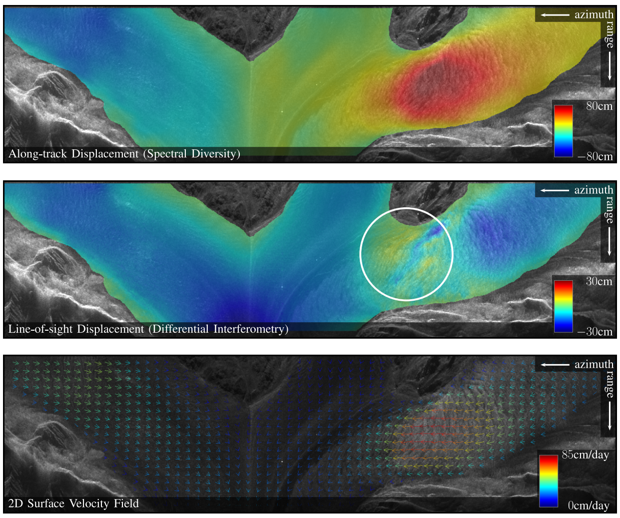

Figure 2: Retrieval of the 2D SVF. FISA configuration, L-band, 2003 campaign.

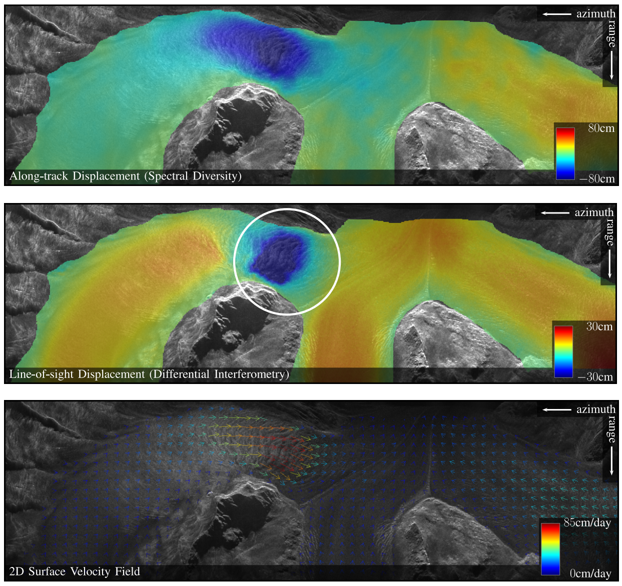

Figure 3: Retrieval of the 2D SVF. FISA configuration, L-band, 2006 campaign.

The areas circled in white in the LOS displacement images of these two figures show a clear example where the acquisition in different configurations allows a better estimation of the glacier motion. In the 2003 campaign the flight configuration resulted in a LOS vector almost perpendicular to the motion vector, resulting in an almost zero motion measurement. However, this is not the case in the 2006 campaign, where the movement of the area going away from the sensor can be clearly observed. **Figure 4**(left) shows the retrieved 3D SVF at L-band for the 2006 campaign in the FISA configuration.

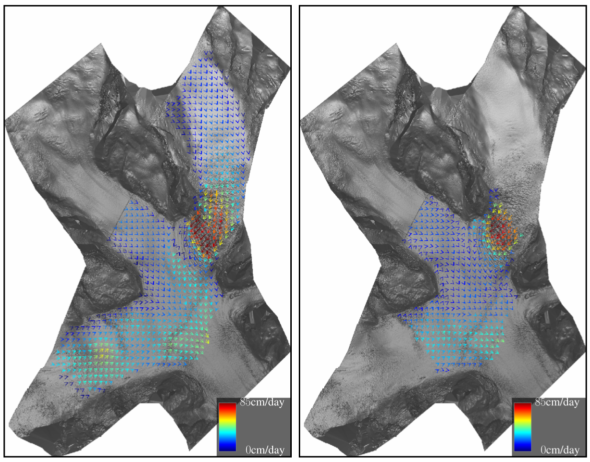

Figure 4: Estimated SVF at L-band in UTM coordinates derived from (left) the 2006 FISA acquisition and (right) the combination of both FISA and JUJO 2006 acquisitions.

The accuracy of the proposed approach can be evaluated using the positions of the CRs deployed in the scene, which were measured using differential GPS. For the 2003 campaign the position of the only CR was measured the 22nd of October and the 5th of November, so that a mean displacement was computed for the motion in cm/day. In the 2006 campaign, the measurements were performed within ± 2 hours of the data acquisitions. The left image of **Figure 5** shows the measurements with respect to the GPS ones for each DInSAR group in the azimuth and slant-range plane, while the right image shows them in UTM coordinates.

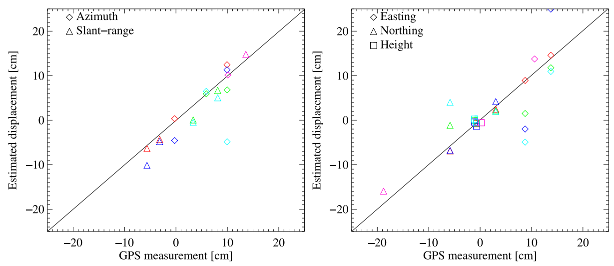

Figure 5: Estimated motion versus GPS measurement for the CRs in (left) the azimuth/slant-range and (right) UTM coordinates. The colors stand for the different configurations: (red) FISA L-band 2006, (green) JUJO L-band 2006, (blue) FISA P-band 2006, (cyan) JUJO P-band 2006, (magenta) FISA L-band 2003.

As commented in Section 3, the combination of different acquisition configurations is possible. The FISA and JUJO configurations of 2006 were combined to obtain the 3D SVF without considering the slope [see Figure 4(right)]. The combination using only the more accurate DInSAR measurement from each configuration was also performed (note that in this case the slope is needed again). **Figure 6** shows the measurements in the CRs after combining the information in these two different ways. Again, results show a good agreement with the in-situ measurements, and note that using the DInSAR measurement alone improves the accuracy of the result mostly in the P-band case.

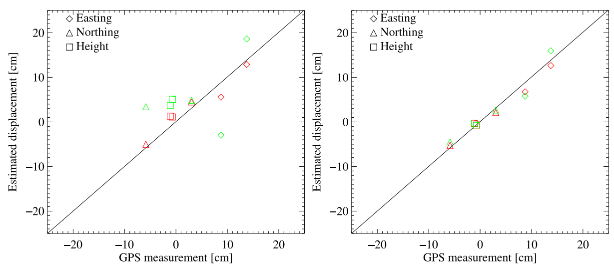

Figure 6: Estimated motion versus GPS measurement for the CRs when combining the FISA and JUJO configurations at (red) L- and (green) P-band, (left) using all four available measurements (no slope used) and (right) using only the DInSAR estimations plus the slope.

5 Conclusion

This paper has shown the possibility to retrieve the 2D and 3D SVF of a glacier using airborne SAR interferometry. An extended multi-squint approach has been proposed to separate the contribution due to RME and TCE. The methodology to efficiently retrieve the SVF using airborne SAR interferometry has been expounded next. All the steps, from SAR processing until the reconstruction of the 3D SVF have been detailed. The presented results together with the evaluation using the CRs deployed in the scene, which resulted in an accuracy in the derived SVF better than 2cm/day rms at L-band, allow to validate the proposed methodology, hence opening a new possibility to monitor temperate glaciers. Future work will address alternative approaches to estimate RME, like the use of autofocus techniques using isolated or point-like scatterers. Also, the analysis of the derived SVF as input to glacier flow models will be subject of future studies.

Acknowledgments

The authors would like to thank the RSL team of University of Zürich for campaign preparation and ground measurements and the E-SAR team of DLR for the flights. The SWISAR campaign was performed with funding of "armasuisse" Switzerland.

References

[1] M. Lüthi and M. Funk: *Dating ice cores from a high Alpine glacier with a flow model for cold firn*, Annals of Glaciology, 31 (1), Jan. 2000.

[2] E. Trouvé *et al.*: *Combining Airborne Photographs and Spaceborne SAR Data to Monitor Temperate Glaciers: Potentials and Limits*, IEEE Trans. Geosci. Remote Sensing, 45 (4), Apr. 2007.

[3] T. Strozzi *et al.*: *Surface Velocity of Swiss Alpine Glaciers from ERS SAR Interferometry*, Proc. of the ENVISAT Symposium, Apr. 2007.

[4] A. Reigber *et al.*: *Refined estimation of time-varying baseline errors in airborne SAR interferometry*, IEEE Geosci. Remote Sensing Lett., 3 (1), Jan. 2006.

[5] R. Scheiber and A. Moreira: *Coregistration of interferometric SAR images using spectral diversity*, IEEE Trans. Geosci. Remote Sensing, 38 (5), Jul. 2000.

[6] A. Moreira *et al.*: *Extended chirp scaling algorithm for air- and spaceborne SAR data processing in stripmap and scanSAR imaging modes*, IEEE Trans. Geosci. Remote Sensing, 34 (5), Sep. 1996.

[7] P. Prats *et al.*: *Comparison of Topography- and Aperture Dependent Motion Compensation Algorithms for Airborne SAR*, IEEE Geosci. Remote Sensing Lett., 4 (3), Jul. 2007.

[8] P. Prats *et al.*: *Glacier Displacement Field Estimation Using Airborne SAR Interferometry*, Proc. IGARSS, Jul. 2007.

[9] P. Prats *et al.*: *Estimation of the Temporal Evolution of the Deformation Using Airborne Differential SAR Interferometry*, IEEE Trans. Geosci. Remote Sensing, 46 (4), Apr. 2008.